https://doi.org/10.5194/acp-2020-99
Preprint. Discussion started: 10 February 2020

Atmospheric Chemistry and Physics Discussions

The Aarhus Chamber Campaign on Highly Oxidized Multifunctional Organic Molecules and Aerosols (ACCHA): Particle Formation and Detailed Chemical Composition at Different Temperatures

Kasper Kristensen[1], Louise N. Jensen[2], Lauriane. L. J. Quéléver[3], Sigurd Christiansen[2], Bernadette Rosati[2,4], Jonas Elm[2], Ricky Teiwes[4], Henrik B. Pedersen[4], Marianne Glasius[2], Mikael Ehn[3], Merete Bilde[2]

[1]Department of Engineering, Aarhus University, 8000 Aarhus C, Denmark
[2]Department of Chemistry and iClimate, Aarhus University, 8000 Aarhus C, Denmark
[3]Institute for Atmospheric and Earth System Research – INAR / Physics, P.O. Box 64, FI-00014, University of Helsinki, Finland
[4]Department of Physics and Astronomy, Aarhus University, 8000 Aarhus C, Denmark

Correspondence to: Kasper Kristensen (kasper.kristensen@eng.au.dk) and Merete Bilde (bilde@chem.au.dk)

Abstract

Little is known about the effects of low temperatures on the formation of SOA from α-pinene. In the current work, ozone-initiated oxidation of α-pinene at initial concentrations of 10 and 50 ppb, respectively, is performed at temperatures of 20, 0 and -15 °C in the Aarhus University Research on Aerosol (AURA) smog chamber during the Aarhus Chamber Campaign on highly oxidized multifunctional organic molecules and Aerosol (ACCHA). Here, we show how temperature influences the formation and chemical composition of α-pinene-derived SOA with a specific focus on the formation of organic acids and dimer esters. With respect to particle formation, results show significant increase in both particle formation rates, particle number concentrations and particle mass concentrations at lower temperatures. In particular, the number concentrations of sub-10 nm particles were significantly enhanced at the lower 0 and -15 °C temperatures. Temperatures also affect chemical composition of the formed SOA. Here, detailed off-line chemical analyses show organic acids contributing from 15 to 30 % by mass, with highest contributions observed at the lower temperatures indicative of enhanced condensation of these semi-volatile species. In comparison, 30 identified dimer esters contribute between 4 – 11 % to SOA mass. No significant differences in the chemical composition (i.e. organic acids and dimer esters) of the α-pinene-derived SOA particles are observed between experiments performed at 10 and 50 ppb initial α-pinene concentrations, thus suggesting a higher influence of reaction temperature compared to that of α-pinene loading on the SOA chemical composition. Interestingly, the effect of temperature on the formation of dimer esters differs between the individual species. The formation of less oxidized (oxygen-to-carbon ratio (O:C) < 0.4) dimer esters is shown to increase at lower temperatures while the formation of the more oxidized (O:C > 0.4) species is suppressed, consequently resulting in temperature-modulated composition of the α-pinene derived SOA. Temperature ramping experiments exposing α-pinene-derived SOA to changing temperatures (heating and cooling) reveal that the chemical composition of the SOA with respect to dimer esters is governed almost solely by the temperature during the initial oxidization and insusceptible to subsequent changes in temperature. Similarly, the resulting SOA mass concentrations were found to be more influenced by the initial α-pinene oxidation temperatures, thus suggesting that the formation conditions to a large extent govern the type of SOA formed, rather than the conditions to which the SOA is later exposed.

For the first time, we discuss the relation between the identified dimer ester and the highly oxidized multifunctional organic molecules (HOMs) measured by Chemical Ionization Atmospheric Pressure interface Time-of-Flight mass spectrometer (CI-APi-TOF) during ACCHA experiments. We propose that, although very different in chemical structures and O:C-ratios, dimer esters and HOMs may be linked through the mechanism of RO_2 autoxidation, and that dimer esters and HOMs merely represent two different fates of the RO_2 radicals.

https://doi.org/10.5194/acp-2020-99
Preprint. Discussion started: 10 February 2020

Atmospheric Chemistry and Physics Discussions

1. Introduction

The oxidation of volatile organic compounds (VOC) constitutes an important source of secondary organic aerosol in the atmosphere. Due to its atmospheric reactivity and its high estimated global emission rate of ~30 Tg/yr (Sindelarova et al., 2014), the atmospheric oxidation of the biogenic VOC α-pinene has been widely studied. The boreal forests are considered abundant sources of α-pinene with varying but sizeable emissions occurring all year around (Hakola et al., 2003;Hakola et al., 2009;Noe et al., 2012). For this reason, the oxidation of α-pinene and subsequent formation of secondary organic aerosol (SOA) is expected to occur at conditions with a wide range of VOC concentrations and atmospheric temperatures.

A number of smog chamber studies have investigated the effect of α-pinene concentration and reaction temperature on the formation of SOA from α-pinene oxidation (Svendby et al., 2008;Pathak et al., 2007;Tillmann et al., 2010;Warren et al., 2009;Kourtchev et al., 2016b;Kristensen et al., 2017). Most of the published studies, however, focus on SOA mass yield (defined as mass of SOA formed per mass of reacted VOC) and reports higher yields with increasing VOC concentrations and lower temperatures. The effect of subzero temperatures, on gas phase oxidation products, nucleation, particle growth and particle chemical composition, remains a largely unexplored area (Huang et al., 2018;Stolzenburg et al., 2018).

Once emitted to the atmosphere, α-pinene is oxidized through reactions with atmospheric oxidants such as ozone (O_3), hydroxyl ($OH^{\cdot}$) and nitrate ($NO_3^{\cdot}$) radicals. These reactions have been shown to result in numerous oxidation products with various chemical functionalities, including alcohols, aldehydes, ketones, carboxylic acids, peroxides and peroxy-acids. As a result of their lower volatilities, many α-pinene derived oxidation products (e.g. carboxylic acids) partition to already existing particles in the atmosphere contributing to particle growth and increased SOA mass. The extent to which an organic compound undergoes partitioning is related to its saturation vapor pressure and to the available particle mass (Kroll and Seinfeld, 2008). Due to the temperature dependence of the saturation vapor pressures of organic oxidation products, higher SOA mass yields from increased condensation of organics are observed at lower temperatures (Pathak et al., 2007;Saathoff et al., 2009;Warren et al., 2009;Svendby et al., 2008).

The saturation vapor pressure of a given organic species is closely related to its chemical structure. Depending on their specific molecular structure and the amount of strong hydrogen bond donor-acceptor groups, the products of α-pinene oxidation may undergo condensation or, if sufficiently low volatile, nucleation, with the latter resulting in new particle formation (Kulmala et al., 2013;Riccobono et al., 2014). Multiple studies report on new particle formation arising from the oxidation of α-pinene and suggest the formation of so-called extremely low volatile organic compounds (ELVOC, Donahue et al. (2012b)) capable of gas-to-particle conversion (Bonn and Moorgat, 2002;Lee and Kamens, 2005;Gao et al., 2010;Tolocka et al., 2006;Claeys et al., 2009;Ehn et al., 2014;Metzger et al., 2010;Kirkby et al., 2016;Bianchi et al., 2019). Although the chemical composition of α-pinene SOA has been extensively studied, uncertainty still remains regarding the chemical structure and functional groups of the compounds responsible for nucleation. Recent quantum chemical results indicate that multi carboxylic acids with three or more acid moieties are some of the most likely compounds to participate in new particle formation (Elm et al., 2017; Elm et al., 2019).

Recently, highly oxidized multifunctional organic molecules (HOMs) have been identified in α-pinene oxidation studies (Bianchi et al., 2019;Ehn et al., 2014;Jokinen et al., 2014;Rissanen et al., 2015). Formed via a gas-phase autoxidation mechanism (Crounse et al., 2013) involving intramolecular hydrogen abstraction by peroxy-radicals, HOMs represent a class of organic compounds which can promptly reach high degrees of oxygenation (Ehn et al., 2017). Oxygen-to-carbon (O:C) ratios exceeding unity have been reported for monomeric compounds (Mutzel et al., 2015;Ehn et al., 2014). The high O:C ratios are attributed to multiple hydroperoxide functionalities and the compounds have been perceived as likely candidates for nucleation and initial particle growth owing to their low volatilities (Tröstl et al., 2016;Kirkby et al., 2016). However, computational studies have shown that HOMs originating from α-pinene autoxidation can have surprisingly high vapor

https://doi.org/10.5194/acp-2020-99
Preprint. Discussion started: 10 February 2020

Atmospheric Chemistry and Physics Discussions

pressures considering their O:C ratios, and it is mainly the dimeric compounds that are likely to be classified as ELVOC (Kurtén et al., 2016;Peräkylä et al., 2019).

High molecular weight (MW > 300 Da) dimer esters formed from oxidation of α-pinene have been identified in laboratory-generated and ambient air SOA (Hoffmann et al., 1998;Tolocka et al., 2004;Gao et al., 2004;Yasmeen et al., 2010;Witkowski and Gierczak, 2014;Kourtchev et al., 2015;Zhang et al., 2015;Kristensen et al., 2013;Kristensen et al., 2014;Kristensen et al., 2016;Kristensen et al., 2017;Mohr et al., 2017). Several mechanisms for the formation of dimer esters have been proposed, including gas-phase mechanisms such as clustering of carboxylic acids (Hoffmann et al., 1998;Claeys et al., 2009;DePalma et al., 2013) and reactions involving reactive intermediates such as stabilized Criegee intermediates (SCI) and RO_2 species (Kristensen et al., 2016;Zhang et al., 2015;Berndt et al., 2016;Witkowski and Gierczak, 2014;Zhao et al., 2015;Kahnt et al., 2018).

The high abundance of dimer esters detected in freshly formed α-pinene derived SOA particles (Kristensen et al., 2016) suggests that these compounds may be important for the initial formation and growth of atmospheric particles; a hypothesis supported by saturation vapor pressure estimates reported in Kristensen et al. (2017) classifying dimer esters as ELVOC with vapor pressures suitable for gas-to-particle phase conversion at room temperatures. Furthermore, recent studies show that dimer esters and other oligomeric compounds in atmospheric aerosol are strongly correlated with cloud condensation nuclei activity thus suggesting a significant impact on climate (Kourtchev et al., 2016).

In contrast to dimer esters, few studies have identified particle phase HOMs and thus their fate upon gas-particle partitioning remains elusive. Recently, Zhang et al. (2017) identified highly oxidized monomers ($C_{8\text{-}10}H_{12\text{-}18}O_{4\text{-}9}$) and dimers ($C_{16\text{-}20}H_{24\text{-}36}O_{8\text{-}14}$) in α-pinene derived SOA particles using Na^+ attachment during electrospray ionization. The dimers identified by Zhang et al. (2017) show a somewhat different chemical formula and degree of oxidation than the gas-phase HOM dimers previously identified by Ehn et al. (2014), where the observed dimer composition was $C_{19\text{-}20}H_{28\text{-}32}O_{11\text{-}18}$. This can be attributed to decomposition of the hydroperoxides functionality of HOMs from processes such as photolysis, thermolysis and solvation, yielding alkoxy radicals, esters, and other moieties. The chemical formulas of the dimeric compounds in Zhang et al. (2017) show good resemblance to the dimer esters published in Kristensen et al. (2016), characterized as $C_{15\text{-}19}H_{24\text{-}30}O_{5\text{-}10}$. This raises the important question, how different types of identified dimers, including HOMs and dimer esters, are related via gas-particle partitioning, chemical reactions or other processes.

The Aarhus Chamber Campaign on HOMs and Aerosols (ACCHA) presented in this work was designed s to elucidate the formation of HOMs and dimer esters from the dark ozonolysis of α-pinene at different temperatures. The effect of temperature and α-pinene concentration on SOA formation and composition on the formation of HOMs and dimer esters is investigated through a series of chamber experiments at temperatures prevailing at the latitudes of the boreal forests (Hakola et al., 2009) i.e. from 20 to -15 °C.

The results of ACCHA are presented in multiple publications. The elemental composition of the bulk α-pinene SOA by High Resolution Time-of-Flight Aerosol Mass Spectrometer (HR-ToF-AMS) is reported in the companion paper by Jensen et al (2019). A study presenting factor analysis of PTR-ToF-MS data includes a case study from the ACCHA campaign (Rosati et al., 2019). The formation of gas-phase HOMs as measured by nitric acid-based Chemical Ionization Atmospheric Pressure interface Time of Flight (CI-APi-ToF) mass spectrometer is presented in the work by Quéléver et al. (2019).

In the current work, we present the effect of temperature and α-pinene concentrations on the formation and molecular composition of SOA particles formed from ozone-initiated oxidation of α-pinene. Specifically, we investigate the contributions of organic acids and dimer esters to α-pinene SOA formed at temeratures of 20, 0, and -15 °C and examine the changes in molecular composition arising from heating and cooling of SOA particles.

https://doi.org/10.5194/acp-2020-99
Preprint. Discussion started: 10 February 2020

Atmospheric Chemistry and Physics Discussions

2. Method

2.1 Chamber experiments

Dark ozonolysis of α-pinene was conducted in the Aarhus University Research on Aerosol (AURA) smog chamber. The chamber is described in detail in Kristensen et al. (2017). In short, the AURA chamber consists of a 5 m^3 Teflon bag situated in a 27 m^3 temperature controlled cold room. The chamber temperature can be varied from -16 °C to +26 °C. The temperature and relative humidity are monitored in the center of the Teflon bag by a HC02 probe coupled to a HygroFlex HF320 transmitter (Rotronic AG, Switzerland). In the current study, the chamber was operated using dry purified air (active carbon, Hepa) at atmospheric pressure. Ozone (O_3, ~100 ppb) was added to the chamber using an ozone generator (Model 610, Jelight Company, Inc.) and the concentration of O_3 and oxides of nitrogen (NO_x) were monitored by UV photometric (O342 Module, Environment S.A.) and chemiluminescent monitors (AC32M, Environment S.A.), respectively. A known amount of VOC was added to a 10 mL glass manifold, evaporated and transferred to the chamber through a stainless-steel inlet (Diameter = 10 mm, Length = 100 cm) using heated (70 °C) N_2-flow. The concentration of the added VOC was monitored using a Gas Chromatograph with Flame Ionization Detector (Agilent 7820A GC-FID, with a time resolution of 6 min) and a Proton Transfer Reaction Time-of-Flight Mass Spectrometer (PTR-ToF- 783 MS 8000; IONICON, Innsbruck, Austria) sampling through stainless steel outlets located opposite of the VOC inlet (distance between inlet and outlet ~ 1.6 m). Particle size distributions were measured using a scanning mobility particle sizer (SMPS) system including a Kr-85 neutralizer (TSI 3077A) and an electrostatic classifier (TSI 3082) coupled with a nano water-based condensation particle counter (CPC, TSI 3788). The SMPS system was optimized for measurements of particles in the range of 10 – 400 nm with a sampling time of 80 s (60 s upscan, 20 s downscan, aerosol flow rate = 1.6 L min^{-1} , sheath flow rate = 5 L min^{-1}). In addition, the total particle number concentration of particles with diameter (D_p) larger than ~1.4 nm was measured by a Particle Size Magnifier (PSM A10, Airmodus, (Vanhanen et al., 2011), sample flow = 2.5 L min^{-1}, time resolution = 1 s) operated in fixed saturator flow mode.

The chemical composition of gas-phase HOMs were measured using a nitric acid-based Chemical Ionization Atmospheric Pressure interface Time-of-Flight mass spectrometer (CI-APi-ToF, Tofwerk A.G., Switzerland / Aerodyne Research Inc., USA) presented by Junninen et al. (2010) and Jokinen et al. (2012). An Aerodyne High-Resolution Time-of-Flight Aerosol Mass Spectrometer (HR-ToF-AMS, Aerodyne Research Inc., (DeCarlo et al., 2006)) was deployed to measure real-time, non-refractory particulate matter. In addition, SOA molecular composition with respect to organic acids and high-molecular-weight dimer esters was investigated through off-line filter analysis of the formed α-pinene derived SOA performed using an Ultra High-Performance Liquid Chromatograph coupled to the electrospray ionization source of a Bruker Daltonics quadrupole time-of-flight mass spectrometer (UHPLC/ESI-qToF-MS). Filter sampling was performed once no additional growth in SOA mass was evident from the SMPS and no α-pinene could be detected by the GC-FID. All filter samples were collected by a low volume sampler onto 47 mm 0.20 micrometer PTFE filters (Advantec) situated in stainless steel filter holders at a flow rate of ~27 L min^{-1} once no additional growth in SOA mass was evident from the SMPS and no α-pinene could be detected by the GC-FID. After collection, the filter samples were stored at -20 °C until extraction and analysis.

A total of 12 α-pinene oxidation experiments conducted in the AURA smog chamber are presented here (Table 1). Each experiment was performed at temperatures close to either 20, 0 or -15 °C to investigate the effect of temperature on the formation and composition of both gas and particle phase organics from dark ozonolysis of α-pinene. Five experiments were conducted with the injection of 10 ppb α-pinene (~0.32 µL, 99%, Sigma Aldrich, Exp. 1.1-1.5) into the ozone-filled chamber (~100 ppb O_3). These experiments include oxidation at constant temperatures 20, 0 and -15 °C (Exp. 1.1, 1.2 and 1.3) and two temperature ramp experiments (Exp. 1.4 and 1.5). The ramp experiments were performed by injection of α-pinene at a fixed 20 °C (Exp. 1.4) or -15 °C (Exp. 1.5) temperature followed by subsequent ramping to -15 or 20 °C, respectively. In both experiments the temperature ramping was initiated approximately 40 min after the injection of α-pinene. In Exp. 1.4 a decrease

https://doi.org/10.5194/acp-2020-99
Preprint. Discussion started: 10 February 2020

Atmospheric Chemistry and Physics Discussions

in temperature from 20 °C to -15 °C was achieved in ~ 100 min, while in Exp. 1.5 heating of the chamber from -15 °C to 20 °C was performed in ~ 140 min.

To investigate the effect of α-pinene concentration on the SOA formation and composition three experiments were performed with 50 ppb of α-pinene (~1.6 µL, 99%, Sigma Aldrich) at 20, 0 and -15 °C (Exp. 2.1-2.3).

The injection of α-pinene in the 10 and 50 ppb experiments described above (Exp. 1.1-2.3) was conducted with a N_2 flow rate of 15 L min^{-1}. To examine the effect of the injection flow rate, the 50 ppb α-pinene Exp. 2.1-2.3 were repeated using an N_2 injection flow of 30 L min^{-1} (Exp. 3.1-3.3).

Throughout this paper SOA density is assumed to be 1 g cm^{-3} as in Kristensen et al. (2017).

2.2 Off-line particle analysis by UHPLC/ESI-qTOF-MS

Collected particle filter samples were extracted and analyzed for organic acids and dimer esters. Filter extraction was performed using a 1:1 mixture of methanol and acetonitrile (HPLC grade, Sigma Aldrich). 0.2 µg of camphoric acid recovery standard was added to the filter sample prior to the addition of the extraction mixture. The samples were placed in a cooled ultrasonic bath for 15 min after which the filters were removed and the extracts filtered through a Teflon filter (0.45 µm pore size, Chromafil). The extraction solvents were then removed by evaporation over gentle N_2 flow and the residues were dissolved by adding 0.2 mL MilliQ water with 10 % acetonitrile and 0.1 % acetic acid. The reconstituted samples were placed in a cooled ultrasonic bath for 5 min and the extract transferred to a HPLC sample vial for analysis. To ensure complete transfer of organics from the evaporated extracts, additional reconstitution were performed with 0.2 mL MilliQ water with 50 % acetonitrile and 0.1 % acetic acid. Both sample solutions (10 % and 50 % acetonitrile reconstitution) were analyzed by UHPLC/ESI-qTOF-MS immediately after extraction.

The HPLC stationary phase was a Waters Acquity UPLC Ethylene Bridged Hybrid C18 column (2.1 x 100 mm 1.7 um) while the mobile phase consisted of acetic acid 0.1% (v/v) in MilliQ water (eluent A) and acetic acid 0.1% (v/v) in acetonitrile as eluent B. The operating conditions of the mass spectrometer have been described elsewhere (Kristensen and Glasius, 2011).

Quantification of the organic acids was performed from eight-level calibration curves (0.1 to 10.0 µg mL^{-1}) of the following acids: cis-pinic, cis-pinonic acid, terpenylic acid, diaterpenylic acid acetate (DTAA), 3-methyl-butane tricarboxylic acid (MBTCA). Due to lack of authentic standards, the dimer esters were quantified using DTAA as surrogate standard.

3. Results and discussions

A representative example of the results obtained from the conducted smog chamber experiments is shown in Fig. 1. Following injection of α-pinene into the ozone-filled chamber at constant temperature and RH, rapid particle formation is captured by the PSM (measuring particles >1.4 nm) and, shortly after, the SMPS (10-400 nm). In all conducted experiments, maximum particle number concentrations were obtained within 10 minutes after α-pinene injection followed by decay ascribed to wall loss and particle aggregation. Particle number concentrations shown in Fig. 1 (lower panel) are wall-loss corrected. During the course of the experiment, decrease in ozone and α-pinene concentration is accompanied by increase in particle SOA mass concentration as measured by the SMPS. Figure 1 (upper panel) shows wall-loss-corrected SOA mass concentration obtained from ozone-initiated oxidation of 50 ppb α-pinene (measured by GC-FID). Wall loss corrections were based on first order fits to the SOA mass or number concentration after peak. The grey shaded area represents the time of filter sampling for off-line chemical analysis by UHPLC/ESI-qTOF-MS. Similar figures showing data from all conducted experiments are presented in Supplementary Information.

https://doi.org/10.5194/acp-2020-99
Preprint. Discussion started: 10 February 2020

Atmospheric Chemistry and Physics Discussions

3.1 Particle formation rates and SOA mass yields

Figure 2A-B show the total particle number concentration (# cm^{-3}) as measured by the PSM (D_p> 1.4 nm) at 20, 0 and -15 °C as a function of time after injection of 10 ppb and 50 ppb α-pinene, respectively. The maximum total particle number concentrations in all experiments are listed in Table 1. Particle formation in terms of number concentrations from the dark ozonolysis of α-pinene at both 10 ppb and 50 ppb VOC concentrations show negative dependence on temperature as has also been reported previously (Jonsson et al., 2008;Kristensen et al., 2017). Maximum particle formation rates (# cm^{-3} s^{-1}) are estimated from linear fits to the experimental time series of total particle number concentration measured by the PSM (Fig. 2A-B inserts). It is clear that lower temperatures result in higher particle formation rates from ozone-initiated oxidation of α-pinene at both low (10 ppb) and high (50 ppb) VOC concentration. At both α-pinene concentrations, a significantly higher particle formation rate is observed when oxidation takes place at 0 °C compared to oxidation performed at 20 °C, with the formation rates being ~ 6 and ~ 20 times higher at 0 °C than at 20 °C, at 10 ppb and 50 ppb α-pinene experiments, respectively. In comparison, the maximum particle formation rate at both α-pinene concentrations only increased by a factor of 1.5 when performing the oxidation at -15 °C compared to 0 °C.

Figures 2C-D show the evolution of the wall-loss-corrected SOA mass concentration (μg m^{-3}) measured by SMPS as a function of time after α-pinene injection. Agreeing with previous studies, SOA mass and mass yields are higher at lower temperatures (Jonsson et al., 2008;Saathoff et al., 2009;Pathak et al., 2007;Kristensen et al., 2017). The reported 18 and 43 % mass yields at 20 °C and -15 °C, respectively, (50 ppb α-pinene, 100 ppb O_3) are in excellent agreement with previous values of 21 % and 39 % from similar oxidation experiments (50 ppb α -pinene, 200 ppb O_3) performed in the same chamber (Kristensen et al., 2017). Compared to experiments performed at 20 °C, temperatures of 0 °C and -15 °C respectively result in ~ 50 % and ~ 150 % higher SOA mass concentrations. Interestingly, SOA mass concentration in both 10 and 50 ppb α-pinene oxidation experiments show almost identical response to temperature going from reaction temperatures of 20 °C to -15 °C. In Fig. 2C and 2D the maximum SOA mass is obtained faster at higher reaction temperatures than at lower temperatures. For both low (10 ppb) and high (50 ppb) α-pinene loadings, maximum SOA mass is reached after approximately 140 min, 200 min and 250 min after α-pinene injection at 20, 0 and -15 °C, respectively. This is attributed to the faster reaction of α-pinene with ozone at higher temperatures, which is also evident from the calculated α-pinene loss rates shown in the insert in Fig. 2D (50 ppb, GC-FID derived; due to the detection limit of the GC-FID no loss rates could be calculated for 10 ppb α-pinene experiments). Compared to oxidation experiments performed at 20 °C, loss rates of α-pinene were found to be 11 % and 22 % lower at 0 °C and -15 °C reaction temperature, respectively. These results are in good agreement with temperature dependent reaction rates of ozone with α-pinene reported by Atkinson et al. (1982) predicting a 16 (± 4) % and 28 (± 6) % lower reaction rate at 0 °C and -15 °C, respectively, relative to the reaction rate calculated at 20 °C. The discrepancy between measured and literature-derived values is likely due to the presence of OH radicals in the current study. Despite the lower reaction rate for α-pinene ozonolysis at low temperature, the particle number concentration data, in Fig. 2, show significantly faster particle formation in cold experiments.

3.2 Particle size distributions and sub-10 nm particles

Figure 3A shows the particle size distributions as recorded by the SMPS after max. SOA mass concentration was reached in (10 ppb) and high (50 ppb) concentration α-pinene oxidation experiments at 20, 0 and -15 °C. At both α-pinene concentrations, lower reaction temperatures result in larger particles consistent with the higher SOA masses at 0 °C and -15 °C in Fig. 3C and 3D. The time evolutions of the particle size distribution measured over time (Fig. 3B) shows that particles formed at 20 °C are initially larger than the particles formed at the two lower temperatures (0 °C and -15 °C). However, during the course of the experiments, particles formed at the lower temperatures grow more rapidly to larger sizes compared to particles formed at 20 °C. This is likely attributable to enhanced condensation of organics onto the formed particles at lower temperatures.

https://doi.org/10.5194/acp-2020-99
Preprint. Discussion started: 10 February 2020

Atmospheric Chemistry and Physics Discussions

Figure 4A shows the total particle number concentration (# cm^{-3}) obtained by the PSM (D_p> 1.4 nm) and SMPS (D_p in the range 10-400 nm) respectively as a function of time after α-pinene injection (10 ppb) at both 20 and -15 °C. The differences in the total particle number concentrations derived by the two instruments corresponds to the number concentrations in the size range of 1.4 nm to 10 nm. Comparing experiments performed at 20, 0 and -15 °C temperatures in Fig. 4B (10 ppb α-pinene), it is clear that the presence of sub-10 nm particles is higher at the lower reaction temperatures and that the largest temperature dependence is in the range 20 °C to 0 °C.

According to Fig. 4A, sub-10 nm particles constitute ~10 and 25 % of the total particle number concentration at 20 and -15 °C, respectively, even 30 min after α-pinene injection where particle number concentrations have peaked. The size distributions obtained from the SMPS (Fig. 4C), however, indicating very few particles in the smaller size-ranges (i.e. below 20 nm, Fig. 4C insert) at this time of the experiments. A possible explanation for the high sub-10 nm particle number concentration is the presence of a particle distribution mode below the detectable range of the SMPS. Supporting this, Lee et al. (2016) reported an absence of particles in the size range between 3 and 8 nm in ambient air particle measurements (1-600 nm particle size distribution range combining PSM and SMPS data) during the Southern Oxidant and Aerosol Study (SOAS) field campaign. To our knowledge, the current work represents the first indication of this observed "gap" in the particle size distribution in smog chamber experiments, thus emphasizing the need for further studies of sub-10 nm particle formation and detection from VOC oxidation.

3.3 Molecular composition

Figure 5 shows the detailed chemical composition of SOA with respect to organic acids and dimer esters at different temperatures (20 °C, 0 °C, and -15 °C) and at two different concentrations of α-pinene (10 ppb and 50 ppb, respectively). The acids and dimer esters identified are similar to those in Kristensen et al. (2017), where suggestions for molecular structures are given. Significantly higher particle concentrations of α-pinene-derived organic acids are evident at the lower 0 and -15 °C temperatures compared to 20 °C supporting increased condensation of organics at lower temperatures. The total contributions of the identified acids to the formed SOA mass in experiments with an initial α-pinene concentration of 10 ppb are 17 %, 25 % and 32 % at 20, 0 and -15 °C, respectively. In comparison, in 50 ppb α-pinene oxidation experiments, the acids contribute to the formed SOA with 18 %, 38 % and 28 % respectively. For comparison, the fraction of acids was 20 % at 20 °C and 31 % at -15 °C of total SOA mass in experiments with 50 ppb of α-pinene and 200 ppb of ozone (Kristensen et al. 2017). Comparing mass fractions of acids at 20 °C and -15 °C, the mass fraction seems to be highly dependent on temperature and much less dependent on VOC concentration or VOC:O_3 ratios.

In all experiments, pinic acid was found to be the dominant identified organic acid, constituting between 5 and 9 % of the formed SOA mass with highest contributions at lower reaction temperatures. A negative dependence of concentration with temperature is observed for six of the ten identified organic acids: pinonic acid, pinalic acid, oxopinonic acid, OH-pinonic acid, pinic acid and terpenylic acid. Diaterpenylic acid acetate (DTAA), diaterpenylic acid (DTA) and 3-methyl-butanetricarboxylic acid (MBTCA), however, show lower concentrations at the lower temperatures compared to at 20 °C. The effect of temperature seems to correlate with the O:C ratio (i.e. degree of oxidation of the organic acids) as shown in Fig. 5. Acids with lower O:C-ratios (O:C < 0.4) are found at higher concentrations at lower temperatures (0 and -15 °C). This can likely be attributed to an enhanced condensation of these species onto the SOA particles at temperatures of 0 and -15 °C. In contrast, although contributing significantly less to the SOA mass, the more oxidized compounds (O:C > 0.4, DTAA, DTA and MBTCA) show an opposite trend with respect to temperature (Fig. S3). As MBTCA, DTAA and DTA are hypothesized to be formed from gas-phase oxidations involving OH-radicals (Szmigielski et al., 2007;Vereecken et al., 2007;Müller et al., 2012;Kristensen et al., 2014), their lower concentrations at lower reaction temperatures could be explained by (1) changes in reaction pathways or branching of the intermediates of MBTCA, DTAA and DTA, (2) lower gas-phase concentration of the first generation of oxidized organic compounds due to higher degree of condensation (e.g. MBTCA is formed from gas-phase

https://doi.org/10.5194/acp-2020-99
Preprint. Discussion started: 10 February 2020

Atmospheric Chemistry and Physics Discussions

oxidation of pinonic acid), and (3) reduction of OH radical production and hence reduced oxidation by OH-radicals at lower reaction temperatures (Jonsson et al., 2008;Tillmann et al., 2010). The former (1) is supported by Müller et al. (2012) and Donahue et al. (2012a) reporting lower particle-phase MBTCA correlating with decreased pinonic acid vapor fractions at lower temperatures. Both explanations are supported by lower O:C ratios of the total α-pinene-derived SOA formed at the lower temperatures as reported in Jensen et al. (2020).

A total of 30 dimer esters were identified in the collected SOA particle samples, from both 10 and 50 ppb α-pinene ozonolysis experiments. In the 10 ppb α-pinene experiments, total concentrations of dimer esters of 0.64, 0.51 and 0.46 μg m^{-3} were found in SOA particles formed at 20, 0 and -15 °C, respectively, thus showing a small positive dependence on temperature. The corresponding mass fractions were: 11.1 %, 7.5 % and 3.8 %. For particles formed from higher 50 ppb α-pinene concentrations, the temperature dependence is less obvious with total dimer ester concentration of 3.1, 4.3, and 3.3 μg m^{-3} at 20, 0, and -15 °C, respectively. The corresponding mass fractions of the dimer esters are: 8.9 %, 8.0 % and 3.9 %, thus similar to fractions reported for the 10 ppb α-pinene oxidation experiments, thus, as in the case of the organic acids, the mass fraction of dimer esters seems to be highly dependent on temperature and much less dependent on VOC concentrations or VOC:O_3 ratios. This is somewhat contradictory to previously published findings by Kourtchev et al. (2016) showing increased particle fraction of oligomeric compounds at higher VOC precursor concentrations.

Looking at the concentrations of the (30) individual dimer esters, their formation is affected differently by the reaction temperature. As an example, the particle-phase concentration of the MW368 dimer ester (pinonyl-pinyl ester, $C_{19}H_{28}O_7$) is increases at lower temperatures, while the opposite is seen for the MW358 dimer esters (pinyl-diaterpenyl ester, $C_{17}H_{26}O_8$). Figure 6A shows the yields of the identified dimer esters at -15 ° C relative to 20 °C (yield (-15 °C) / yield (20 °C)) as a function of the number of carbon atoms in the dimer esters. From this, it is clear that the effect of temperature on the formation of individual dimer esters is compound specific. Of the 30 dimer esters, increased particle concentrations at lower temperatures is most often related to species with high carbon number (i.e. C_{19} species). Also, Fig. 6A shows that the temperature effect on the dimer ester concentration to a large extent depends on the O:C ratio (indicated by color scale) of the individual species. This is highlighted also in Fig. 6B showing a more significant decrease in relative yields of dimer esters with higher oxygen number (i.e. more oxidized) at the lower -15 °C temperature in both 10 and 50 ppb α-pinene experiments. Accordingly, the dimer esters are grouped based on their O:C ratios, with the more oxidized dimer esters having an O:C > 0.4. The total concentrations of the low (< 0.4) and high (> 0.4) O:C dimer esters are shown in Fig. 5B and 5D inserts. Recently, gas-phase RO_2–RO_2 reactions followed by particle phase decomposition of the resulting diacyl peroxides have been suggested as a possible mechanism for the formation of dimer esters from α-pinene ozonolysis (Zhang et al., 2015). As the decomposition of diacyl peroxides and the subsequent formation of dimer esters is suggested to increase at higher temperatures, this could indicate that the formation of the high O:C dimer esters proceed through the suggested RO_2-RO_2 reaction pathway, thus explaining increased concentrations at higher temperatures. Also, it is worth considering that the lower O:C dimer esters (such as the MW368 pinonyl-pinyl ester) may be composed of diacyl peroxides or acyloxyalkyl hydroperoxides, thus explaining the observed increased concentrations of these species at the lower temperatures owing to the suggested unstable nature of hydroperoxide-containing compounds (Krapf et al., 2016) .

Thermodynamics also need to be considered as possible explanation for the observed temperature responses of the high and low O:C dimer esters. As reported in Kristensen et al. (2017), the identified dimer esters span across a wide range of volatilities. Here, many of the low O:C dimer esters may be sufficiently volatile to allow considerable fractions to exist in the gas phase at high temperature. Consequently, the increased particle-phase concentration observed at the lower temperatures may solely be attributed to enhanced gas-to-particle phase partitioning of these species. Supporting this, Mohr et al. (2017) identified dimeric monoterpene oxidation products ($C_{16–20}H_yO_{6–9}$) in both particle and gas phases in ambient air measurements in the boreal forest in Finland.

https://doi.org/10.5194/acp-2020-99
Preprint. Discussion started: 10 February 2020

Atmospheric Chemistry and Physics Discussions

325 **3.4 Temperature ramping**

Normann Jensen et al. (2020) present a detailed analysis on changes in AMS derived elemental chemical composition during temperature ramps in the ACCHA campaign and show that temperature at which the particles are formed to a large extend determines the elemental composition also after subsequent heating or cooling by 35 °C. During two temperature ramp experiments, we also studied how the concentration, mass fraction and molar yields of carboxylic acids and dimer esters as
330 identified in the off-line analysis varied. The experiments involving temperature ramps were conducted to examine whether the observed effect of temperature on the dimer ester concentration is attributed to gas-to-particle partitioning or stabilization/decomposition of the hydroperoxide-containing species.

Figure 7A shows the SOA mass formation (wall-loss corrected) from the 10 ppb α-pinene oxidation experiments performed at constant 20 °C (Exp. 1.1) and -15 °C (Exp. 1.3) and from the two temperature ramping experiments (Exp. 1.4 and 1.5) in which
335 the chamber temperature was ramped up or down ~ 40 min after injection of α-pinene. In the ~ 40 min following the injection of α-pinene, SOA mass in both ramp experiments show good agreement with the constant temperature experiments performed at similar starting temperature (Exp. 1.1 and 1.3). Likewise, particle formation rate and maximum particle number concentration obtained in Exp. 1.4 and 1.5 prior to temperature changes (Table 1) also resembles that of Exp. 1.1 and 1.3. Thus the initial evolution of the particle formation in Exp. 1.1 (constant 20 °C) and Exp. 1.4 (ramp experiment initiated at 20 °C)
340 and experiment 1.3 (constant -15°C) and Exp. 1.5 (ramp experiment initiated at -15 °C) are comparable.

From Fig. 7A, cooling and heating the chamber imply a quasi-immediate effect on the SOA mass concentration. In Exp. 1.4, decreasing the temperature results in a maximum SOA mass concentration being ~ 30 % higher than the maximum SOA mass in Exp. 1.1 performed at a constant 20 °C (8 versus 6 µg m^{-3}). Reversely, heating the chamber from -15 to 20 °C (Exp. 1.5) results in a ~ 30 % lower SOA mass (10 versus 15 µg m^{-3}) compared to SOA formed and kept at -15 °C (Exp. 1.3). The changes
345 in particle size distributions as a result of temperature ramping (Fig. 7B) are attributed to evaporation during heating and condensation during cooling. Interestingly, despite the loss or gain of particle mass during temperature ramping the SOA mass concentration is closer to the experiments performed at the initial temperature rather than the final temperature even after a temperature ramp of 35 °C. This, in turn, suggests that the formation conditions to a large extent govern the type of SOA that was formed, rather than the conditions the SOA was later exposed to.

350 Figure 8 shows the concentrations, mass fractions and molar yields of organic acids and dimer esters in SOA particles from constant temperature oxidation experiments at 20 and -15 °C (Exp. 1.1 and 1.3, respectively) and from the two temperature ramp experiments (Exp. 1.4 and 1.5). Upon heating SOA particles from -15 to 20 °C, a loss of particle mass (5 µg m^{-3}, Fig. 7) was observed and is attributed to evaporation of organics. This is supported by a 2.8 µg m^{-3} lower organic acid concentration in particles exposed to heating in Exp. 1.5 compared to particles formed at the constant -15 °C (Exp. 1.3), accounting for ~ 60
355 % of the evaporated organics. These results underline the semi-volatile nature of the identified organic acids (i.e. pinalic acid, pinonic acid, oxopinonic acid, OH-pinonic acid, pinic acid, terpenylic acid and terebic acid) and show that these acids are readily removed from organic aerosols during heating thus explaining previously reported reduced aerosol mass fraction from heating α-pinene SOA (Pathak et al., 2007). Figure 8 reveals that heating and cooling of α-pinene-derived SOA particles results in insignificant or small changes in the concentrations, mass fractions, and molar yields of dimer esters when compared to
360 experiments performed at constant temperatures. This indicates that the dimer esters are not subjected to evaporation or decomposition within the studied temperature range and timeframe. These results show that the concentration of the dimer esters in SOA from α-pinene oxidation is largely determined by the temperature by which the SOA is formed rather than subsequent exposure to higher or lower temperatures.

3.5 Dimer ester formation and HOMs

365 A detailed study on the formation of HOMs during the ACCHA campaign is presented by Quéléver et al. (2019). Here, significantly lower (by orders of magnitude) HOM gas-phase concentrations are observed in -15 °C experiments compared to

https://doi.org/10.5194/acp-2020-99
Preprint. Discussion started: 10 February 2020

Atmospheric Chemistry and Physics Discussions

20 °C experiments. As the HOMs form through autoxidation of RO_2, low temperatures and thus decreased autoxidation is expected to result in lower formation of HOMs, with reduced formation of the more oxygenated species. Interestingly, however, Quéléver et al. (2019) observed no correlation between the degree of oxidation (i.e. O:C-ratio) of the identified HOMs and the magnitude by which the formation of these was reduced at lower temperatures. This is in contrast to the observed temperature effects on the formation of the identified dimer esters presented in the current study (Fig. 7). In Quéléver et al. (2019), one possible interpretation of the observed temperature effect on HOMs is that the rate-limiting step in the autoxidation chain takes place in RO_2 radicals with six or fewer oxygen atoms. This is supported by the observed decreased concentration of dimer esters with a higher number of oxygen atoms, which also indicates that the formation of the identified dimer esters likely proceeds through reaction of RO_2. The observed response to temperature of the different dimer esters may thus be ascribed to the oxidation state of RO_2 species available for gas-phase reactions. At the lower reaction temperatures, the RO_2 autoxidation is limited, thus favoring the formation of low O:C dimer esters through reaction of less oxidized RO_2 species. Likewise, the higher O:C dimer esters thus only form if sufficient degree of autoxidation of the RO_2 is allowed before bimolecular cross-reaction takes place and the dimer esters are formed.

We thus propose that, although different in chemical structures and O:C-ratios, dimer esters and HOMs may be linked through their formation mechanisms, both involving RO_2 autoxidation. The particle-phase dimer esters and the gas-phase HOMs may merely represent two different fates of the RO_2 radicals. If conditions are favorable and efficient autoxidation takes place, this will result in the formation of HOMs, which by the definition recommended by Bianchi et al. (2019) in this case means any molecule with 6 or more oxygen atoms that has undergone autoxidation. On the other hand, dimer esters could be the product of RO_2 cross reactions, with O:C ratios influenced by the number of potential autoxidation steps undertaken by the involved RO_2 species prior to reaction (Fig. 9). In this case, if either RO_2 has undergone autoxidation, the resulting dimers would classify as HOM, regardless whether the ultimate fate is a dimer peroxide or dimer ester. The formation of dimer esters through reactions of RO_2 is supported by an observed decrease in dimer esters concentrations at higher levels of NOx in ambient air measurement in Hyytiälä, Finland (Kristensen et al., 2016) and supports the formation proposed by several studies (Ehn et al., 2014;Berndt et al., 2018;Zhao et al., 2018) involving RO_2 cross-reactions as likely route of gaseous dimer formation.

4. Conclusions

The formation of SOA from dark ozonolysis of α-pinene is highly influenced by temperature. At sub-zero temperatures, such as -15°C, more effective nucleation gives rise to significantly higher particle number concentration compared to similar experiments performed at 20 °C, where the vast majority of laboratory studies are conducted. In addition, the SOA mass concentration resulting from α-pinene ozonolysis shows a strong temperature dependence attributed to increased condensation of semi-volatile oxidation products at lower temperatures. This is supported by higher concentration of semi-volatile organic acids, such as pinic acid and pinonic acid, in SOA particles formed at 0 °C and -15 °C compared to particles formed at 20 °C. In addition to organic acids, the contribution of high-molecular-weight dimer esters to the formed SOA is also affected by temperature. Underlining the chemical complexity of α-pinene SOA, the 30 quantified dimer esters showed different behaviors with respect to temperature, with the suppressed formation of the more oxidized dimer esters (O:C > 0.4) at low reaction temperatures. This feature is not seen in the case of the least oxidized dimer esters (O:C < 0.4), showing a small increase in particle concentration at lower temperatures. Similar to the high O:C dimer ester compounds, α-pinene ozonolysis experiments performed at lower temperatures result in lower HOM formation in the gas-phase. We suggest that the identified dimer esters may form through RO_2 cross-reactions likely involving hydroperoxide-containing compounds from autoxidation. The identification of dimer esters in SOA would thus signify a specific termination pathway and fate of the RO_2 radicals, and link these molecules more close to HOMs than earlier thought. These results indicate that temperature not only affects the formation of SOA mass in the atmosphere but also alters the chemical composition through condensation and evaporation of semi-volatile

https://doi.org/10.5194/acp-2020-99
Preprint. Discussion started: 10 February 2020

Atmospheric Chemistry and Physics Discussions

species, changes in the formation of HOMs and finally in the reaction pathways leading to the formation of dimer esters having high and low O:C-ratios.

With respect to dimer esters, no decomposition or evidence of partitioning changes between the aerosol and the gas phase were observed from heating or cooling the SOA particles, suggesting that 1) the formation and, consequently, concentration of dimer esters is dictated by the VOC oxidation conditions and 2) once formed, dimer esters remain in the particle phase, representing a core compound within SOA and thus an efficient organic carbon binder to the aerosol phase. In relation, the presented results from temperature ramping show that final SOA mass concentration obtained from dark ozonolysis of α-pinene is more dependent on the initial reaction temperatures rather than temperatures to which the formed SOA is subsequently exposed. In conclusion, this means that the changes at ambient temperatures in areas in which emissions and oxidation of VOCs, such as α-pinene, is likely to result in significant changes to the resulting SOA mass as well as the chemical composition of the SOA. As global temperatures are expected to rise, especially in the Nordic regions of the boreal forests, this means that although less SOA mass is expected to form from the oxidation of emitted biogenic VOCs, the temperature-induced changes to the chemical composition may result in more temperature resistant SOA influencing cloud-forming abilities from increased content of oligomeric compounds (i.e. dimer esters).

Author contributions

MB, ME, and MG and HBP supervised the ACCHA campaign. KK, LLJQ, SC, ME, and MB designed the experiments. KK, LNJ, SC initialized the chamber for experiments. KK and LNJ measured and analyzed the aerosol phase. KK, BR, and RT measured and analyzed the VOCs and their oxidation production. LLJQ performed the measurement and analyzed the gas-phase HOMs. JE guided and helped with the interpretation of the dimer ester data and formation pathways. KK prepared the manuscript with the contributions from all co-authors.

Acknowledgement

We thank Aarhus University and Aarhus University Research Foundation for support. This work was supported by the European Research Council (Grant 638703-COALA) and the Academy of Finland (grants 307331, 317380 and 320094). KK acknowledge the Carlsberg Foundation (Grant CF18-0883) for financial support. JE thanks the Villum foundation and the Swedish Research Council Formas project number 2018-01745-COBACCA for financial support.

https://doi.org/10.5194/acp-2020-99
Preprint. Discussion started: 10 February 2020

Atmospheric Chemistry and Physics Discussions

435

Table 1. Overview of conducted α-pinene ozonolysis experiments

ID	Date	Exp. Type	α-pinene (ppb)	α-pinene injection flow (LPM)	Ozone (at injection) (ppb)	Temp. [a] (at injection) (°C)	RH [a] (at injection) (%)	Temp. avg. [b] (°C)	RH avg. [b] (%)	VOC loss rate [c] (h^{-1})	Max SOA mass [d] (μg m^{-3})	Max particle number [d] (10-400nm) (# cm^{-3})	Max particle number (>1.4nm) (# cm^{-3}) [e]
1.1	20161202	Low load, 20 °C	10	15	104	20.2	0	20.3 (±0.1)	0.8 (±0.8)	N/A	6	$3.9 \cdot 10^4$	$5.2 \cdot 10^4$
1.2	20161208	Low load, 0 °C	10	15	105	0.9	2.9	0.7 (±2.7)	7.1 (±4.1)	N/A	9	$7.9 \cdot 10^4$	$17.0 \cdot 10^4$
1.3	20161207	Low load, -15 °C	10	15	106	-13.7	8	-14.7 (±0.1)	12.9 (±5.3)	N/A	15	$7.4 \cdot 10^4$	$19.5 \cdot 10^4$
1.4	20161209	Low load, 20 to -15 °C	10	15	103	19.9	0		N/A	N/A	8	$4.4 \cdot 10^4$	$8.4 \cdot 10^4$
1.5	20161220	Low load, -15 to 20 °C	10	15	113	-14	11.7		5.3 (±4.0)	N/A	10	$9.4 \cdot 10^4$	$20.0 \cdot 10^4$
2.1[∞]	20161212	High load, 20 °C	50	15	105	19.8	0	20 (±1.1)	1.1 (±1.3)	1.0	50	$8.2 \cdot 10^4$	$11.0 \cdot 10^4$
2.2	20161219	High load, 0 °C	50	15	107	-0.4	6.9	-0.3 (±0.1)	6.9 (±0.8)	0.9	65	$19.0 \cdot 10^4$	>$70.0 \cdot 10^4$ *
2.3a	20161213	High load, -15 °C	50	15	101	-13.1	6.7	-14.9 (±0.6)	11.9 (±4.3)	0.8	120	$24.0 \cdot 10^4$	>$70.0 \cdot 10^4$ *
2.3b[∞]	20161221	High load, -15 °C	50	15	113	-14.0	19.8	-15.0 (±0.2)	24.7 (±3.6)	0.8	131	$16.0 \cdot 10^4$	$51.2 \cdot 10^4$
3.1	20170112	High load, 20 °C	50	30	100	20.3	0	20.1 (±0.5)	2.4 (±2.0)	1.1	50	$7.8 \cdot 10^4$	$8.4 \cdot 10^4$
3.2	20170116	High load, 0 °C	50	30	105	0.2	8.6	0.0 (±0.1)	8.7 (±1.1)	1.0	78	$25.0 \cdot 10^4$	>$70.0 \cdot 10^4$ *
3.3	20170113	High load, -15 °C	50	30	105	-14.5	11.2	-14.8 (±0.6)	15.8 (±4.5)	0.9	115	$23.0 \cdot 10^4$	>$70.0 \cdot 10^4$ *

440

[a] Temperature and RH measured in centre of Teflon bag,

[b] Average temperature and RH (±std.dev.) over the entire experiment,

[c] VOC loss rates are estimated from GC-FID measurements

[d] Measured by SMPS (10-400nm), [e] Measured by PSM (>1.4nm),

445 * PSM overloaded

∞ Temperature ramps were performed after the stable temperature phase and is presented in Jensen et al., (2019).

https://doi.org/10.5194/acp-2020-99
Preprint. Discussion started: 10 February 2020

Atmospheric Chemistry and Physics Discussions

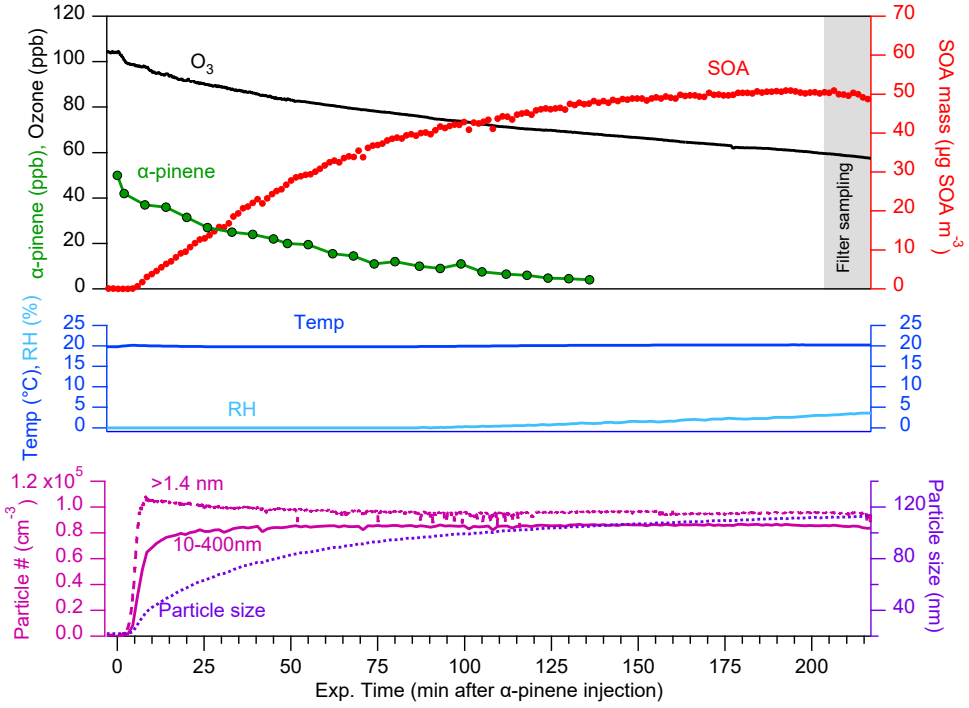

Figure 1. Concentration of O_3 (ppb, black), α-pinene (ppb, green), wall-loss corrected SOA mass (µg m-3, red) and particle number concentration (# cm^{-3}, measured by PSM (>1.4nm) and SMPS (10-400nm), dark red) and the geometric mean particle size (nm, by SMPS, violet) along with recorded RH (%, teal) and temperature (°C, blue) during a 50 ppb α-pinene oxidation experiment performed at 20 °C (Exp. 2.1).

https://doi.org/10.5194/acp-2020-99
Preprint. Discussion started: 10 February 2020

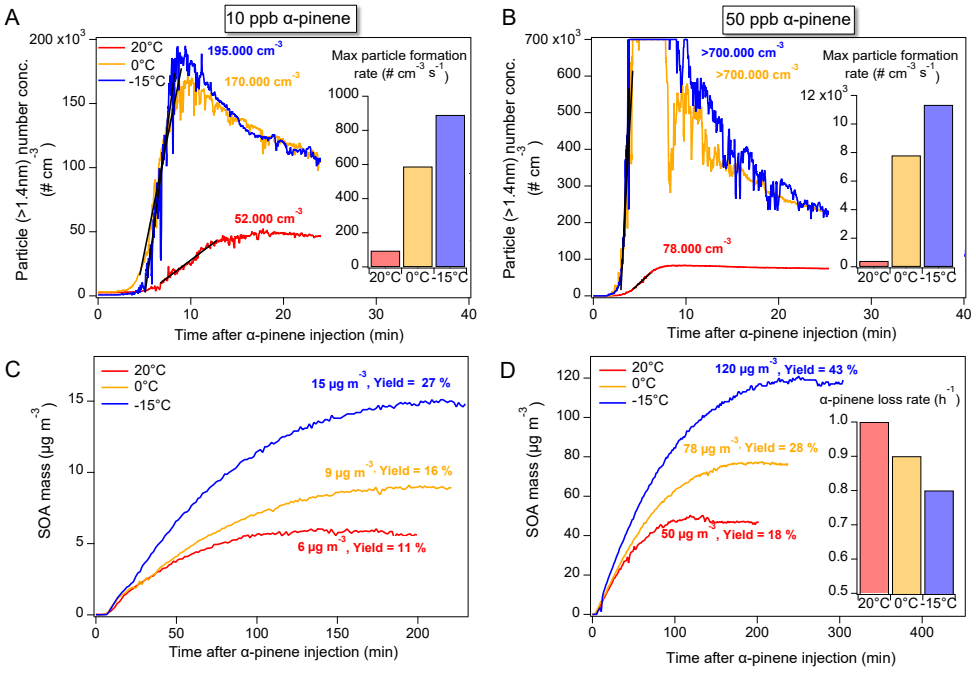

Figure 2. Effect of reaction temperature and initial VOC loading on SOA formation: Particle number concentration (A, B) and wall-loss-corrected SOA mass concentration (C, D) at α-pinene concentrations of 10 ppb (A, C) and 50 ppb (B, D). Inserts show particle formation rates (# cm^{-3} s^{-1}) as estimated from linear fits to the experimental data (A, B). The insert in D shows the loss rate of α-pinene (h^{-1}) at different temperatures as derived from an exponential fit to the measured concentration of α-pinene.

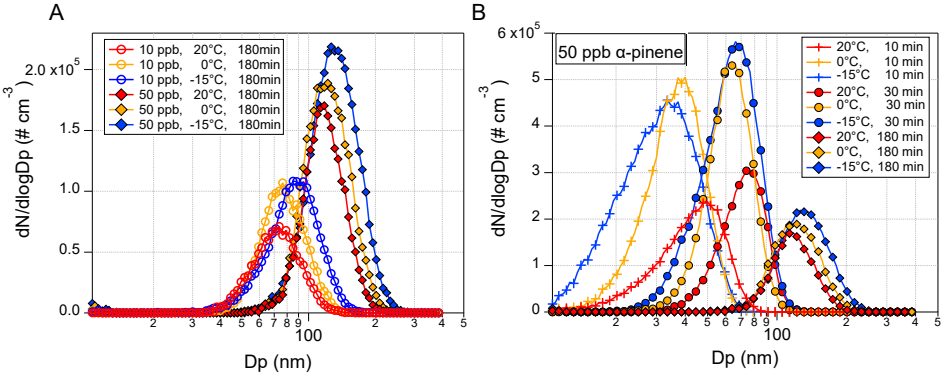

Figure 3. **A)** Particle size distribution recorded 180 minutes after the ozone-initiated oxidation of 10 (Exp. 1.1-1.3) and 50 ppb (Exp. 2.1-2.3) α-pinene performed at 20 °C (red), 0 °C (orange), and -15 °C (blue). **B)** Particle size distribution recorded at 10, 30 and 180 minutes after injection of 50 ppb α-pinene at 20 °C (Exp. 2.1, red), 0 °C (Exp. 2.2, orange), and -15 °C (Exp. 2.3, blue).

https://doi.org/10.5194/acp-2020-99
Preprint. Discussion started: 10 February 2020

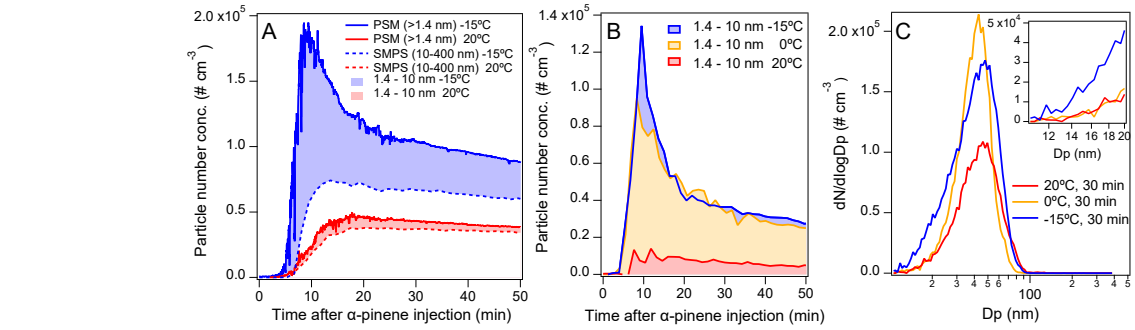

Figure 4. **A)** Effect of temperature on particle number concentrations (# cm^{-3}) as derived from the SMPS (10-400 nm particle size range, broken line) and PSM (>1.4 nm particle size range, solid line) in experiments with an initial α-pinene concentration of 10 ppb. (Exp. 1.1, red, and Exp. 1.3, blue). **B)** Particle number concentrations (# cm^{-3}) of 1.4 – 10 nm particles in experiments with an initial α-pinene concentration of 10 ppb performed at -15°, 0 °C and 20 °C (Exp. 1.1, 1.2, and 1.3, respectively). **C)** Particle size distributions recorded 30 minutes after the ozone-initiated oxidation of 10 ppb α-pinene performed at 20 °C (red), 0 °C (orange), and -15 °C (blue) (Exp. 1.1-1.3).

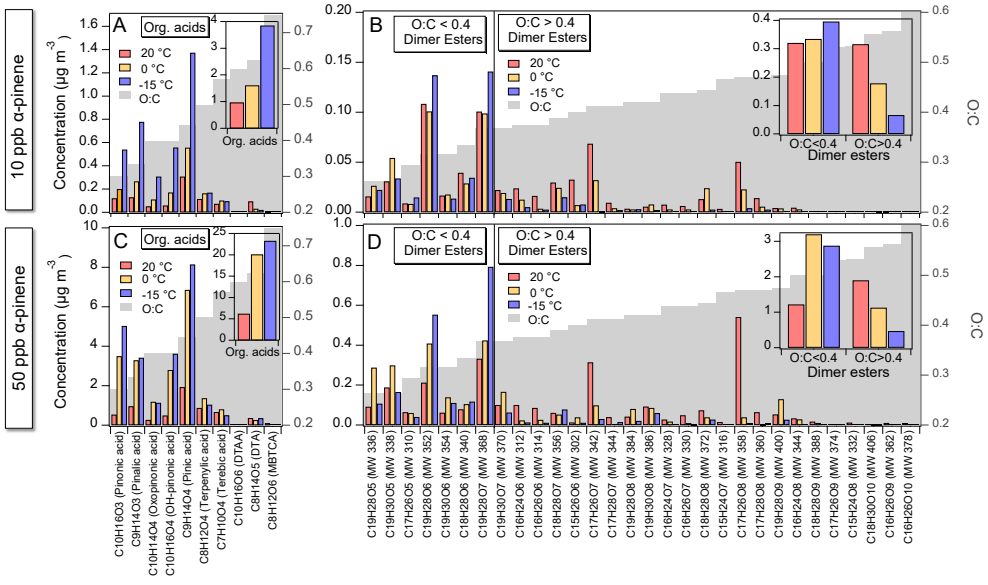

Figure 5. LC-MS results showing concentrations (µg m^{-3}, left axis) of acids and dimer etsers as well as O:C ratios (grey bars, right axis) of these at 20 °C (red), 0 °C (orange), and -15 °C (blue) for the two α-pinene loadings; 10 ppb (top panels **A** and **B**), 50 ppb (bottom panels **C** and **D**). Inserts show the total concentrations of the identified organic acids and dimer esters (O:C < 0.4 and O:C > 0.4)

https://doi.org/10.5194/acp-2020-99
Preprint. Discussion started: 10 February 2020

Atmospheric Chemistry and Physics Discussions

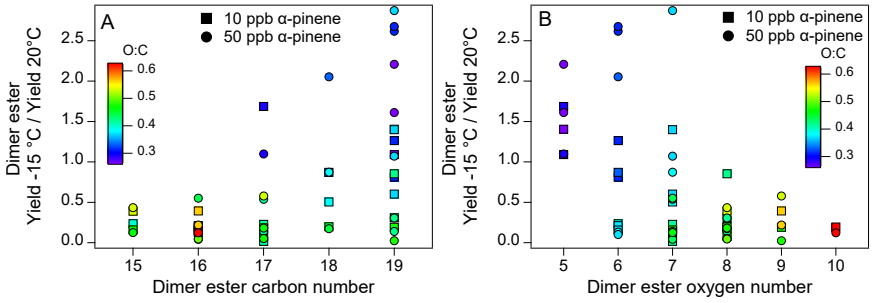

480 **Figure 6.** Comparison of relative yields (yield at -15 °C / yields at 20 °C) for specific dimer esters as a function of dimer ester carbon number (**A**) and oxygen number (**B**) in 10 and 50 ppb α-pinene ozonolysis experiments. Color scale indicates the O:C ratio of the dimer esters.

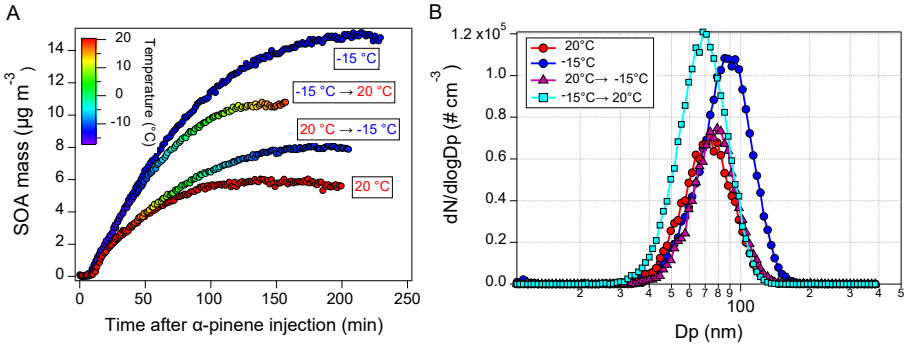

Figure 7. Effect of ramping temperature (20 °C → -15 °C, Exp. 1.4, and -15 °C → 20 °C, Exp. 1.5) on the wall-loss corrected
485 SOA mass concentration (**A**) and final particle size distribution (**B**) from ozonolysis of 10 ppb α-pinene. For comparison, results from constant -15 °C and 20°C temperature experiments (Exp. 1.1 and Exp. 1.3, respectively) are also shown.

https://doi.org/10.5194/acp-2020-99
Preprint. Discussion started: 10 February 2020

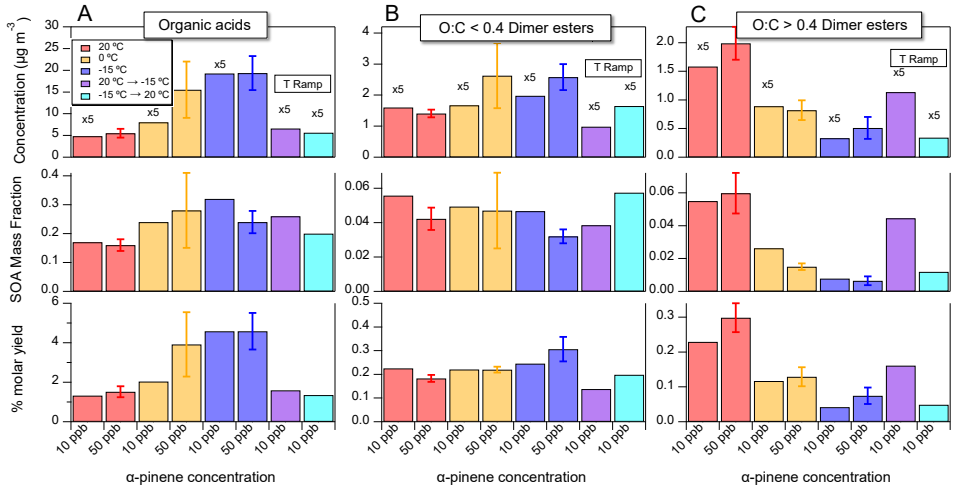

Figure 8. Effect of α-pinene concentration and temperature on the mass concentrations (µg m-3), SOA mass fractions, and molar yield of the identified organic acids (column A), low O:C (<0.4) dimer esters (column B) and high O:C (>0.4) dimer esters (column C). Note that the concentrations (µg m-3) of organic acids and dimer esters related to the 10 ppb α-pinene oxidation experiments have been multiplied with a factor of 5 (top panels). For the 50 ppb pinene oxidation experiments average values are reported from Exp. 2.1-2.3 and Exp. 3.1-3.3. Error bars represent one standard deviation.

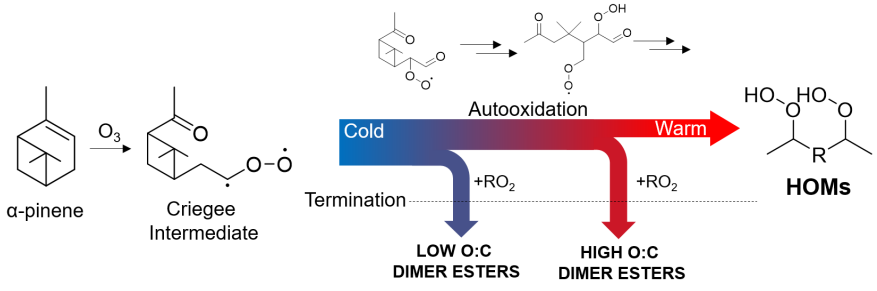

Figure 9. Illustration of the proposed relation between low O:C (< 0.4) and high O:C (> 0.4) dimer ester formation and HOMs.

https://doi.org/10.5194/acp-2020-99
Preprint. Discussion started: 10 February 2020

Atmospheric Chemistry and Physics Discussions

References

Atkinson, R., Winer, A. M., and Pitts, J. N.: Rate constants for the gas phase reactions of O3 with the natural hydrocarbons isoprene and α- and β-pinene, Atmos. Environ., 16, 1017-1020, 1982.

Berndt, T., Richters, S., Jokinen, T., Hyttinen, N., Kurtén, T., Otkjær, R. V., Kjaergaard, H. G., Stratmann, F., Herrmann, H., and Sipilä, M.: Hydroxyl radical-induced formation of highly oxidized organic compounds, Nat. Commun,, 7, 13677, 2016.

Berndt, T., Scholz, W., Mentler, B., Fischer, L., Herrmann, H., Kulmala, M., and Hansel, A.: Accretion Product Formation from Self- and Cross-Reactions of RO2 Radicals in the Atmosphere, Angew. Chem. Int. Ed., 57, 3820-3824, 2018.

Bianchi, F., Kurtén, T., Riva, M., Mohr, C., Rissanen, M. P., Roldin, P., Berndt, T., Crounse, J. D., Wennberg, P. O., Mentel, T. F., Wildt, J., Junninen, H., Jokinen, T., Kulmala, M., Worsnop, D. R., Thornton, J. A., Donahue, N., Kjaergaard, H. G., and Ehn, M.: Highly Oxygenated Organic Molecules (HOM) from Gas-Phase Autoxidation Involving Peroxy Radicals: A Key Contributor to Atmospheric Aerosol, Chem. Rev., 119, 3472-3509, 2019.

Bonn, B., and Moorgat, G.: New particle formation during a-and b-pinene oxidation by O 3, OH and NO 3, and the influence of water vapour: particle size distribution studies, Atmos. Chem. Phys., 2, 183-196, 2002.

Claeys, M., Iinuma, Y., Szmigielski, R., Surratt, J. D., Blockhuys, F., Van Alsenoy, C., Boege, O., Sierau, B., Gomez-Gonzalez, Y., Vermeylen, R., Van der Veken, P., Shahgholi, M., Chan, A. W. H., Herrmann, H., Seinfeld, J. H., and Maenhaut, W.: Terpenylic Acid and Related Compounds from the Oxidation of alpha-Pinene: Implications for New Particle Formation and Growth above Forests, Environ. Sci. Technol., 43, 6976-6982, 2009.

Crounse, J. D., Nielsen, L. B., Jørgensen, S., Kjaergaard, H. G., and Wennberg, P. O.: Autoxidation of Organic Compounds in the Atmosphere, J. Phys. Chem. Lett., 4, 3513-3520, 2013.

DeCarlo, P. F., Kimmel, J. R., Trimborn, A., Northway, M. J., Jayne, J. T., Aiken, A. C., Gonin, M., Fuhrer, K., Horvath, T., Docherty, K. S., Worsnop, D. R., and Jimenez, J. L.: Field-Deployable, High-Resolution, Time-of-Flight Aerosol Mass Spectrometer, Anal Chem, 78, 8281-8289, 2006.

DePalma, J. W., Horan, A. J., Hall Iv, W. A., and Johnston, M. V.: Thermodynamics of oligomer formation: implications for secondary organic aerosol formation and reactivity, Phys Chem Chem Phys, 15, 6935-6944, 2013.

Donahue, N. M., Henry, K. M., Mentel, T. F., Kiendler-Scharr, A., Spindler, C., Bohn, B., Brauers, T., Dorn, H. P., Fuchs, H., and Tillmann, R.: Aging of biogenic secondary organic aerosol via gas-phase OH radical reactions, Proc. Natl. Acad. Sci., 109, 13503-13508, 2012a.

Donahue, N. M., Kroll, J., Pandis, S. N., and Robinson, A. L.: A two-dimensional volatility basis set–Part 2: Diagnostics of organic-aerosol evolution, Atmos. Chem. Phys., 12, 615-634, 2012b.

Ehn, M., Thornton, J. A., Kleist, E., Sipilä, M., Junninen, H., Pullinen, I., Springer, M., Rubach, F., Tillmann, R., and Lee, B.: A large source of low-volatility secondary organic aerosol, Nature, 506, 476, 2014.

Ehn, M., Berndt, T., Wildt, J., and Mentel, T.: Highly Oxygenated Molecules from Atmospheric Autoxidation of Hydrocarbons: A Prominent Challenge for Chemical Kinetics Studies, Int J Chem Kinet, 49, 821-831, 2017.

Elm, J., Myllys, N., and Kurtén, T.: What Is Required for Highly Oxidized Molecules To Form Clusters with Sulfuric Acid?, J. Phys. Chem. A, 121, 4578-4587, 10.1021/acs.jpca.7b03759, 2017.

Elm, J.: Unexpected Growth Coordinate in Large Clusters Consisting of Sulfuric Acid and C8H12O6 Tricarboxylic Acid, The J. Phys. Chem. A, 123, 3170-3175, 10.1021/acs.jpca.9b00428, 2019.

https://doi.org/10.5194/acp-2020-99
Preprint. Discussion started: 10 February 2020

Gao, S., Ng, N. L., Keywood, M., Varutbangkul, V., Bahreini, R., Nenes, A., He, J., Yoo, K. Y., Beauchamp, J., and Hodyss, R. P.: Particle phase acidity and oligomer formation in secondary organic aerosol, Environ. Sci. Technol., 38, 6582-6589, 2004.

Gao, Y., Hall, W. A., and Johnston, M. V.: Molecular Composition of Monoterpene Secondary Organic Aerosol at Low Mass Loading, Environ. Sci. Technol., 44, 7897-7902, 2010.

Hakola, H., Tarvainen, V., Laurila, T., Hiltunen, V., Hellén, H., and Keronen, P.: Seasonal variation of VOC concentrations above a boreal coniferous forest, Atmos. Environ., 37, 1623-1634, 2003.

Hakola, H., Hellén, H., Tarvainen, V., Bäck, J., Patokoski, J., and Rinne, J.: Annual variations of atmospheric VOC concentrations in a boreal forest, Boreal Environ. Res, 14, 722-730, 2009.

Hoffmann, T., Bandur, R., Marggraf, U., and Linscheid, M.: Molecular composition of organic aerosols formed in the alpha-pinene/O-3 reaction: Implications for new particle formation processes, J. Geophys. Res.: Atmos., 103, 25569-25578, 1998.

Huang, W., Saathoff, H., Pajunoja, A., Shen, X., Naumann, K. H., Wagner, R., Virtanen, A., Leisner, T., and Mohr, C.: α-Pinene secondary organic aerosol at low temperature: chemical composition and implications for particle viscosity, Atmos. Chem. Phys., 18, 2883-2898, 2018.

Jensen L.N., Canagaratna M.R., Kristensen K., Quéléver L. L. J., Rosati B., Teiwes R., Glasius M., Pedersen H. B., Ehn M., Bilde M.: Chemical composition of alpha-pinene derived secondary organic aerosol: Effects of loading and temperature, Submitted to Atmos. Chem. Phys. Discuss., 2020

Jokinen, T., Sipilä, M., Richters, S., Kerminen, V.-M., Paasonen, P., Stratmann, F., Worsnop, D., Kulmala, M., Ehn, M., Herrmann, H., and Berndt, T.: Rapid Autoxidation Forms Highly Oxidized RO2 Radicals in the Atmosphere, Angew. Chem. Int. Ed., 53, 14596-14600, 2014.

Jonsson, Å., Hallquist, M., and Ljungström, E.: The effect of temperature and water on secondary organic aerosol formation from ozonolysis of limonene, Δ 3-carene and α-pinene, Atmos. Chem. Phys., 8, 6541-6549, 2008.

Kahnt, A., Vermeylen, R., Iinuma, Y., Safi Shalamzari, M., Maenhaut, W., and Claeys, M.: High-molecular-weight esters in α-pinene ozonolysis secondary organic aerosol: Structural characterization and mechanistic proposal for their formation from highly oxygenated molecules, Atmos. Chem. Phys., 18, 8453-8467, 2018.

Kirkby, J., Duplissy, J., Sengupta, K., Frege, C., Gordon, H., Williamson, C., Heinritzi, M., Simon, M., Yan, C., Almeida, J., Tröstl, J., Nieminen, T., Ortega, I. K., Wagner, R., Adamov, A., Amorim, A., Bernhammer, A.-K., Bianchi, F., Breitenlechner, M., Brilke, S., Chen, X., Craven, J., Dias, A., Ehrhart, S., Flagan, R. C., Franchin, A., Fuchs, C., Guida, R., Hakala, J., Hoyle, C. R., Jokinen, T., Junninen, H., Kangasluoma, J., Kim, J., Krapf, M., Kürten, A., Laaksonen, A., Lehtipalo, K., Makhmutov, V., Mathot, S., Molteni, U., Onnela, A., Peräkylä, O., Piel, F., Petäjä, T., Praplan, A. P., Pringle, K., Rap, A., Richards, N. A. D., Riipinen, I., Rissanen, M. P., Rondo, L., Sarnela, N., Schobesberger, S., Scott, C. E., Seinfeld, J. H., Sipilä, M., Steiner, G., Stozhkov, Y., Stratmann, F., Tomé, A., Virtanen, A., Vogel, A. L., Wagner, A. C., Wagner, P. E., Weingartner, E., Wimmer, D., Winkler, P. M., Ye, P., Zhang, X., Hansel, A., Dommen, J., Donahue, N. M., Worsnop, D. R., Baltensperger, U., Kulmala, M., Carslaw, K. S., and Curtius, J.: Ion-induced nucleation of pure biogenic particles, Nature, 533, 521, 2016.

Kourtchev, I., Doussin, J.-F., Giorio, C., Mahon, B., Wilson, E. M., Maurin, N., Pangui, E., Venables, D. S., Wenger, J. C., and Kalberer, M.: Molecular composition of fresh and aged secondary organic aerosol from a mixture of biogenic volatile compounds: a high-resolution mass spectrometry study, Atmos. Chem. Phys., 15, 5683-5695, 2015.

https://doi.org/10.5194/acp-2020-99
Preprint. Discussion started: 10 February 2020

Kourtchev, I., Giorio, C., Manninen, A., Wilson, E., Mahon, B., Aalto, J., Kajos, M., Venables, D., Ruuskanen, T., and Levula, J.: Enhanced Volatile Organic Compounds emissions and organic aerosol mass increase the oligomer content of atmospheric aerosols, Sci Rep-Uk, 6, 2016.

Krapf, M., El Haddad, I., Bruns, E. A., Molteni, U., Daellenbach, K. R., Prévôt, A. S., Baltensperger, U., and Dommen, J.: Labile peroxides in secondary organic aerosol, Chem, 1, 603-616, 2016.

Kristensen, K., and Glasius, M.: Organosulfates and oxidation products from biogenic hydrocarbons in fine aerosols from a forest in North West Europe during spring, Atmos. Environ., 45, 4546-4556, 2011.

Kristensen, K., Enggrob, K. L., King, S., Worton, D., Platt, S., Mortensen, R., Rosenoern, T., Surratt, J., Bilde, M., and Goldstein, A.: Formation and occurrence of dimer esters of pinene oxidation products in atmospheric aerosols, Atmos. Chem. Phys., 13, 3763-3776, 2013.

Kristensen, K., Cui, T., Zhang, H., Gold, A., Glasius, M., and Surratt, J.: Dimers in α-pinene secondary organic aerosol: effect of hydroxyl radical, ozone, relative humidity and aerosol acidity, Atmos. Chem. Phys., 14, 4201-4218, 2014.

Kristensen, K., Watne, Å. K., Hammes, J., Lutz, A., Petäjä, T., Hallquist, M., Bilde, M., and Glasius, M.: High-Molecular Weight Dimer Esters Are Major Products in Aerosols from α-Pinene Ozonolysis and the Boreal Forest, Environ. Sci. Technol., Lett., 3, 280-285, 2016.

Kristensen, K., Jensen, L., Glasius, M., and Bilde, M.: The effect of sub-zero temperature on the formation and composition of secondary organic aerosol from ozonolysis of alpha-pinene, Environ. Sci.: Process. Impacts 19, 1220-1234, 2017.

Kroll, J. H., and Seinfeld, J. H.: Chemistry of secondary organic aerosol: Formation and evolution of low-volatility organics in the atmosphere, Atmos. Environ., 42, 3593-3624, 2008.

Kulmala, M., Kontkanen, J., Junninen, H., Lehtipalo, K., Manninen, H. E., Nieminen, T., Petäjä, T., Sipilä, M., Schobesberger, S., and Rantala, P.: Direct observations of atmospheric aerosol nucleation, Science, 339, 943-946, 2013.

Kurtén, T., Tiusanen, K., Roldin, P., Rissanen, M., Luy, J.-N., Boy, M., Ehn, M., and Donahue, N.: α-Pinene autoxidation products may not have extremely low saturation vapor pressures despite high O: C ratios, J. Phys. Chem. A, 120, 2569-2582, 2016.

Lee, S., and Kamens, R. M.: Particle nucleation from the reaction of α-pinene and O3, Atmos. Environ., 39, 6822-6832, 2005.

Lee, S. H., Uin, J., Guenther, A. B., de Gouw, J. A., Yu, F., Nadykto, A. B., Herb, J., Ng, N. L., Koss, A., and Brune, W. H.: Isoprene suppression of new particle formation: Potential mechanisms and implications, J. Geophys. Res.: Atmos., 121, 14,621-614,635, 2016.

Metzger, A., Verheggen, B., Dommen, J., Duplissy, J., Prevot, A. S., Weingartner, E., Riipinen, I., Kulmala, M., Spracklen, D. V., and Carslaw, K. S.: Evidence for the role of organics in aerosol particle formation under atmospheric conditions, Proc. Natl. Acad. Sci., 107, 6646-6651, 2010.

Mohr, C., Lopez-Hilfiker, F. D., Yli-Juuti, T., Heitto, A., Lutz, A., Hallquist, M., D'Ambro, E. L., Rissanen, M. P., Hao, L., and Schobesberger, S.: Ambient observations of dimers from terpene oxidation in the gas phase: Implications for new particle formation and growth, Geophys. Res. Lett., 44, 2958-2966, 2017.

Mutzel, A., Poulain, L., Berndt, T., Iinuma, Y., Rodigast, M., Böge, O., Richters, S., Spindler, G., Sipilä, M., Jokinen, T., Kulmala, M., and Herrmann, H.: Highly Oxidized Multifunctional Organic Compounds Observed in Tropospheric Particles: A Field and Laboratory Study, Environ. Sci. Technol., 49, 7754-7761, 2015.

https://doi.org/10.5194/acp-2020-99
Preprint. Discussion started: 10 February 2020

Atmospheric Chemistry and Physics Discussions

Müller, L., Reinnig, M.-C., Naumann, K., Saathoff, H., Mentel, T., Donahue, N., and Hoffmann, T.: Formation of 3-methyl-1, 2, 3-butanetricarboxylic acid via gas phase oxidation of pinonic acid–a mass spectrometric study of SOA aging, Atmos. Chem. Phys., 12, 1483-1496, 2012.

Noe, S., Hüve, K., Niinemets, Ü., and Copolovici, L.: Seasonal variation in vertical volatile compounds air concentrations within a remote hemiboreal mixed forest, Atmos. Chem. Phys., 12, 3909-3926, 2012.

Pathak, R. K., Stanier, C. O., Donahue, N. M., and Pandis, S. N.: Ozonolysis of α-pinene at atmospherically relevant concentrations: Temperature dependence of aerosol mass fractions (yields), J. Geophys. Res.: Atmos., 112, 2007.

Peräkylä, O., Riva, M., Heikkinen, L., Quéléver, L., Roldin, P., and Ehn, M.: Experimental investigation into the volatilities of highly oxygenated organic molecules (HOM), Atmos. Chem. Phys. Discuss., 2019, 1-28, 2019.

Quéléver, L. L., Kristensen, K., Normann Jensen, L., Rosati, B., Teiwes, R., Daellenbach, K. R., Peräkylä, O., Roldin, P., Bossi, R., and Pedersen, H. B.: Effect of temperature on the formation of highly oxygenated organic molecules (HOMs) from alpha-pinene ozonolysis, Atmos. Chem. Phys., 19, 7609-7625, 2019.

Riccobono, F., Schobesberger, S., Scott, C. E., Dommen, J., Ortega, I. K., Rondo, L., Almeida, J., Amorim, A., Bianchi, F., and Breitenlechner, M.: Oxidation products of biogenic emissions contribute to nucleation of atmospheric particles, Science, 344, 717-721, 2014.

Rissanen, M. P., Kurtén, T., Sipilä, M., Thornton, J. A., Kausiala, O., Garmash, O., Kjaergaard, H. G., Petäjä, T., Worsnop, D. R., Ehn, M., and Kulmala, M.: Effects of Chemical Complexity on the Autoxidation Mechanisms of Endocyclic Alkene Ozonolysis Products: From Methylcyclohexenes toward Understanding α-Pinene, J. Phys. Chem. A, 119, 4633-4650, 2015.

Rosati, B., Teiwes, R., Kristensen, K., Bossi, R., Skov, H., Glasius, M., Pedersen, H. B., and Bilde, M.: Factor analysis of chemical ionization experiments: Numerical simulations and an experimental case study of the ozonolysis of α-pinene using a PTR-ToF-MS, Atmos. Environ., 199, 15-31, 2019.

Sindelarova, K., Granier, C., Bouarar, I., Guenther, A., Tilmes, S., Stavrakou, T., Müller, J.-F., Kuhn, U., Stefani, P., and Knorr, W.: Global data set of biogenic VOC emissions calculated by the MEGAN model over the last 30 years, Atmos. Chem. Phys., 14, 9317-9341, 2014.

Stolzenburg, D., Fischer, L., Vogel, A. L., Heinritzi, M., Schervish, M., Simon, M., Wagner, A. C., Dada, L., Ahonen, L. R., Amorim, A., Baccarini, A., Bauer, P. S., Baumgartner, B., Bergen, A., Bianchi, F., Breitenlechner, M., Brilke, S., Buenrostro Mazon, S., Chen, D., Dias, A., Draper, D. C., Duplissy, J., El Haddad, I., Finkenzeller, H., Frege, C., Fuchs, C., Garmash, O., Gordon, H., He, X., Helm, J., Hofbauer, V., Hoyle, C. R., Kim, C., Kirkby, J., Kontkanen, J., Kürten, A., Lampilahti, J., Lawler, M., Lehtipalo, K., Leiminger, M., Mai, H., Mathot, S., Mentler, B., Molteni, U., Nie, W., Nieminen, T., Nowak, J. B., Ojdanic, A., Onnela, A., Passananti, M., Petäjä, T., Quéléver, L. L. J., Rissanen, M. P., Sarnela, N., Schallhart, S., Tauber, C., Tomé, A., Wagner, R., Wang, M., Weitz, L., Wimmer, D., Xiao, M., Yan, C., Ye, P., Zha, Q., Baltensperger, U., Curtius, J., Dommen, J., Flagan, R. C., Kulmala, M., Smith, J. N., Worsnop, D. R., Hansel, A., Donahue, N. M., and Winkler, P. M.: Rapid growth of organic aerosol nanoparticles over a wide tropospheric temperature range, Proc. Natl. Acad. Sci., 115, 9122-9127, 2018.

Svendby, T. M., Lazaridis, M., and Tørseth, K.: Temperature dependent secondary organic aerosol formation from terpenes and aromatics, J. Atmos. Chem., 59, 25-46, 2008.

Szmigielski, R., Surratt, J. D., Gómez-González, Y., Van der Veken, P., Kourtchev, I., Vermeylen, R., Blockhuys, F., Jaoui, M., Kleindienst, T. E., and Lewandowski, M.: 3-methyl-1, 2, 3-butanetricarboxylic acid: An atmospheric tracer for terpene secondary organic aerosol, Geophys, Res. Lett., 34, 2007.

https://doi.org/10.5194/acp-2020-99
Preprint. Discussion started: 10 February 2020

645 Saathoff, H., Naumann, K. H., Möhler, O., Jonsson, Å. M., Hallquist, M., Kiendler-Scharr, A., Mentel, T. F., Tillmann, R., and Schurath, U.: Temperature dependence of yields of secondary organic aerosols from the ozonolysis of α-pinene and limonene, Atmos. Chem. Phys., 9, 1551-1577, 2009.

Tillmann, R., Hallquist, M., Jonsson, Å., Kiendler-Scharr, A., Saathoff, H., Iinuma, Y., and Mentel, T. F.: Influence of relative humidity and temperature on the production of pinonaldehyde and OH radicals from the ozonolysis of α-pinene, Atmos. Chem.
650 Phys., 10, 7057-7072, 2010.

Tolocka, M. P., Jang, M., Ginter, J. M., Cox, F. J., Kamens, R. M., and Johnston, M. V.: Formation of Oligomers in Secondary Organic Aerosol, Environ. Sci. Technol., 38, 1428-1434, 2004.

Tolocka, M. P., Heaton, K. J., Dreyfus, M. A., Wang, S., Zordan, C. A., Saul, T. D., and Johnston, M. V.: Chemistry of Particle Inception and Growth during α-Pinene Ozonolysis, Environ. Sci. Technol., 40, 1843-1848, 2006.

655 Tröstl, J., Chuang, W. K., Gordon, H., Heinritzi, M., Yan, C., Molteni, U., Ahlm, L., Frege, C., Bianchi, F., and Wagner, R.: The role of low-volatility organic compounds in initial particle growth in the atmosphere, Nature, 533, 527, 2016.

Vanhanen, J., Mikkilä, J., Lehtipalo, K., Sipilä, M., Manninen, H. E., Siivola, E., Petäjä, T., and Kulmala, M.: Particle Size Magnifier for Nano-CN Detection, Aerosol Sci. Technol., 45, 533-542, 2011.

Vereecken, L., Müller, J.-F., and Peeters, J.: Low-volatility poly-oxygenates in the OH-initiated atmospheric oxidation of α-
660 pinene: impact of non-traditional peroxyl radical chemistry, Phys Chem Chem Phys, 9, 5241-5248, 2007.

Warren, B., Austin, R. L., and Cocker, D. R.: Temperature dependence of secondary organic aerosol, Atmos. Environ., 43, 3548-3555, 2009.

Witkowski, B., and Gierczak, T.: Early stage composition of SOA produced by alpha-pinene/ozone reaction: alpha-Acyloxyhydroperoxy aldehydes and acidic dimers, Atmos. Environ., 95, 59-70, 2014.

665 Yasmeen, F., Vermeylen, R., Szmigielski, R., Iinuma, Y., Böge, O., Herrmann, H., Maenhaut, W., and Claeys, M.: Terpenylic acid and related compounds: precursors for dimers in secondary organic aerosol from the ozonolysis of α-and β-pinene, Atmos. Chem. Phys., 10, 9383-9392, 2010.

Zhang, X., McVay, R. C., Huang, D. D., Dalleska, N. F., Aumont, B., Flagan, R. C., and Seinfeld, J. H.: Formation and evolution of molecular products in α-pinene secondary organic aerosol, Proc. Natl. Acad. Sci., 112, 14168-14173, 2015.

670 Zhang, X., Lambe, A. T., Upshur, M. A., Brooks, W. A., Gray Bé, A., Thomson, R. J., Geiger, F. M., Surratt, J. D., Zhang, Z., and Gold, A.: Highly oxygenated multifunctional compounds in α-pinene secondary organic aerosol, Environ. Sci. Technol., 51, 5932-5940, 2017.

Zhao, Y., Wingen, L. M., Perraud, V., Greaves, J., and Finlayson-Pitts, B. J.: Role of the reaction of stabilized Criegee intermediates with peroxy radicals in particle formation and growth in air, Phys Chem Chem Phys, 17, 12500-12514, 2015.

675 Zhao, Y., Thornton, J. A., and Pye, H. O.: Quantitative constraints on autoxidation and dimer formation from direct probing of monoterpene-derived peroxy radical chemistry, Proc. Natl. Acad. Sci., 115, 12142-12147, 2018.